PROGRESSIVE DAMAGE MODELING OF CURVED COMPOSITE STRUCTURES FOR OFFLOADING HOSES

Maikson L. P. Tonatto[1*], Maria M. C. Forte[1], Volnei Tita[2], Sandro C. Amico[1]

[1]Post-Graduation Program in Mining, Metallurgical and Materials Engineering, Federal University of Rio Grande do Sul, Porto Alegre, RS, Brazil

[2]Department of Aeronautical Engineering, University of São Paulo, São Carlos, SP, Brazil

*Corresponding author: maikson.tonatto@ufrgs.br

Abstract: Carbon fiber composites have been used for manufacturing curved structures, which are applied in several equipment due to their high specific stiffness and strength. Recently, improvement in pultrusion and filament winding processes allowed the use of curved profile to manufacture coils and rings for selected applications. However, the behavior of these components is complex and hard to predict. In the present work, a progressive damage model is used to simulate the behavior of unidirectional curved structures made of carbon fiber/epoxy intended for marine oil offloading hoses. Tensile, compressive and shear properties of the laminates are used as parameters of the model. For the evaluation of the finite element model, a four-point bending test was carried out on the curved samples instrumented with strain gages. Progressive failure analysis was performed considering the degradation of stiffness, which was reduced until a critical stiffness value in relation to the undamaged sample was reached. A UMAT (User Material subroutine) with the damage model was used to predict progressive failure via Abaqus software. A three-dimensional, non-linear, finite element model considering the same conditions of the four-point bending test was implemented to simulate curved composites (e.g. coils and rings), including failure prediction.

Keywords: Composite structures, progressive damage model, curved components, four-point bending test, oil offloading hoses.

1. INTRODUCTION

The use of composite materials by the naval industry in the structural components has increased due to their high strength and low weight. Interesting applications include pipes, such as risers used in oil production and hoses used for oil offloading. The composite materials may also offer other advantages such as excellent corrosion resistance, low thermal conductivity and good fatigue performance [1]. However, application in this industry is limited due to the complex design and the demanding certification process [2, 3].

The failure process encompasses many phenomena [4], such as fiber fracture, fiber pull out, matrix cracking, fiber debonding, fiber kinking, interface cracks and fiber splitting, all defined as intra-ply failure modes, and it is also common delamination between plies [5]. Simulation tools are important to allow the development of material models able to represent these failure modes and the degradation of the composite structure. There are many models available in the literature, Ribeiro et al. [4] developed a damage model to predict composite structures failure using the mesoscale approach in flat samples. The damage model equations were written and implemented in a user material subroutine (UMAT), in

FORTRAN language, and linked to the commercial FE code (ABAQUS™). The calibration model was based on experimental data to evaluate laminate failure when subjected to triaxial stress. The obtain theoretical data for laminates subjected to several loads has shown generally good agreement with the experimental data. Mayes and Hansen [6] have developed the Multi-Continuum Theory (MCT) which consists in an algorithm embedded in the lamina analysis to decompose lamina stress and strain fields down to the fiber and matrix constituent level. The MCT is a progressive failure analysis related to independent matrix and fiber failures. By using other type of damage model, Almeida Jr. et al. [7] developed a finite element model to predict damage in tubes manufactured by filament winding.

Literature studies involving spirals and rings in composites are particularly scarce, and the models usually predict failure of flat samples (laminates) instead of actual more complex geometries. Indeed, to determine damage behavior of components is necessary to obtained the behavior in other development stages, as represented in the pyramid shown in Figure 1. This work focuses on the calibration of phenomenological models for carbon fiber curved structures (i.e. spiral and rings). To validate the numerical results obtained through Finite Element Analyses (FEA), four-point bending experimental tests were used. A non-linear model was developed to predict damage, stiffness degradation and structural failure of the studied curved structures.

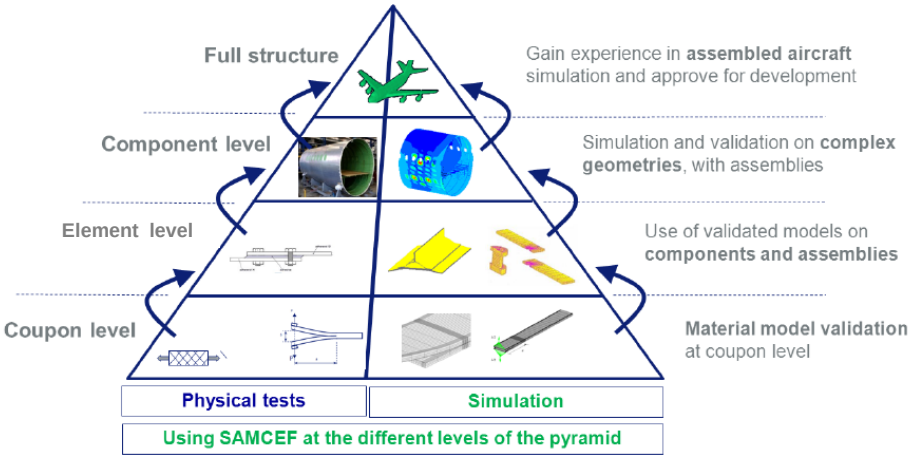

Figure 1: The pyramid of tests, devided in experimental and simulation [5].

2. IDENTIFICATION OF PARAMETERS

Two spiral shaped samples of circular cross section (wire diameter 12.7 mm and pitch 40 mm) were manufactured with epoxy resin and carbon fiber (CF), one by pultrusion (named E/PU/S – epoxy/pultrusion/spiral) and the other one by filament winding (named E/FW/S - epoxy/filament winding/spiral). The third sample was ring-shaped, square cross section of 11 × 11 mm^2, and manufactured with poly(p-phenylene sulfide) (PPS) and carbon fiber by filament winding (named PPS/FW/R - PPS/filament winding/ring). Both spirals and the ring have a middle diameter of 581 mm and the fibers are oriented parallel to the profile (i.e. at 0°). The curved specimens were cut from the spiral and the ring longitudinally to the fiber orientation.

Samples of 340 mm length were cut from the spiral and the rings for testing at LaPol/UFRGS. The American Society for Testing and Materials (ASTM) standards (D4476, D6272 and D7264) were analyzed as parameters due there is not an specific standards to bending test of the curved samples. The four-point bending test (Figure 2(a)) was carried in an Instron 3382. The curved composites were tested with the supports span spaced 100 mm and speed rate of 2 mm/min until failure. Strain measurements were carried out using strain gages strategically positioned as shown in Figure 2(b). A

HBM QuantumX MX1615 data acquisition system was used, with one half bridge with three wires, controlled by software Catman®EASY.

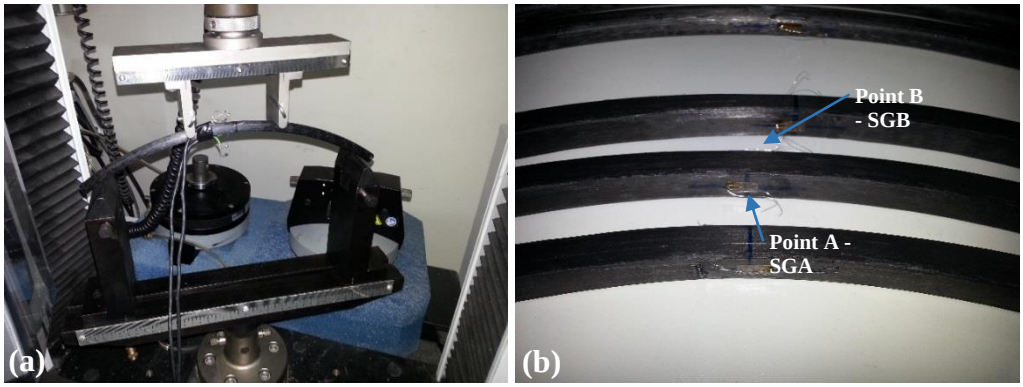

Figure 2: (a) Four-point bending experimental test setup, and (b) curved samples with strain gages.

3. FINITE ELEMENT STRUCTURAL MODELLING

Non-linear FE analyses were carried out using commercial software Abaqus™. The Autodesk Simulation Composite Analysis 2015 plugin was used to evaluate failure criteria and for the implementation of the Multi-Continuum Theory (MCT). This auxiliary program significantly improves speed and accuracy of the model building process. The material properties of the carbon fiber were experimentally measured [8] and are compiled in Table 1.

Table 1: Mechanical properties of the materials [7].

Mechanical properties	***E/PU/S***	***E/FW/S***	***PPS/FW/R***
ρ_c (g/cm³)	1.49	1.43	1.53
V_f (%)	61.3	56.0	54.7
E_{11} (GPa)	116.3	106.9	114.8
$E_{22} = E_{33}$ (GPa)	7.9	7.4	7.8
$\nu_{12} = \nu_{13}$	0.32	0.33	0.35
ν_{23}	0.37	0.37	0.39
$G_{12} = G_{13}$ (GPa)	4.05	3.52	4.07
G_{23} (GPa)	2.87	2.70	2.86
σ^{T}_{11} (MPa)	1878.1	1436.6	1879.6
σ^{T}_{22} (MPa)	59.0	50.0	59.0
σ^{C}_{11} (MPa)	937.0	910.0	897.2
σ^{C}_{22} (MPa)	213.0	210.0	212.0
τ_{12} (MPa)	68.3	52.3	68.1
τ_{13} (MPa)	67.7	38.1	22.6
τ_{23} (MPa)	67.0	66.0	67.0

The structure was modeled with 20-node quadratic hexahedral elements with reduced integration (defined in Abaqus™ as C3D20R). A mesh with 12240 elements and 56571 nodes was selected based on the stabilization of the maximum bending load in the spiral section. The boundary conditions for the four-point bending tests were applied to simulate the condition imposed by the supports. The devices of the four-point bending test are in contact with the sample and it was modelled as analytical rigid body, shown in Figure 3. Reference points (RP) were modelled with the rigid body and the boundary conditions were applied. For the lower device, displacements and rotations in all directions in the reference point were not allowed ($U_x = U_y = U_z = U_{rx} = U_{ry} = U_{rz} = 0$). For the upper device, a displacement in the y direction (green arrow) was applied and the other displacement and rotations in the reference point were not allowed ($U_x = U_z = U_{rx} = U_{ry} = U_{rz} = 0$). It was applied formulation penalty contact with 0.3 coefficient of friction between sample and devices for the tangential interactions and hard contact for the normal interactions. The material orientation of the sample was carried out using cylindrical coordinate system, with fiber direction (local arrow 1) in the same direction of the length geometry. With the same conditions than the spiral section, the ring section was modelled with 6768 elements and 34349 nodes.

Three configurations for the spiral and rings were modelled, varying the mechanical properties, E/PU/S, E/FW/S and PPS/FW/R and the geometry.

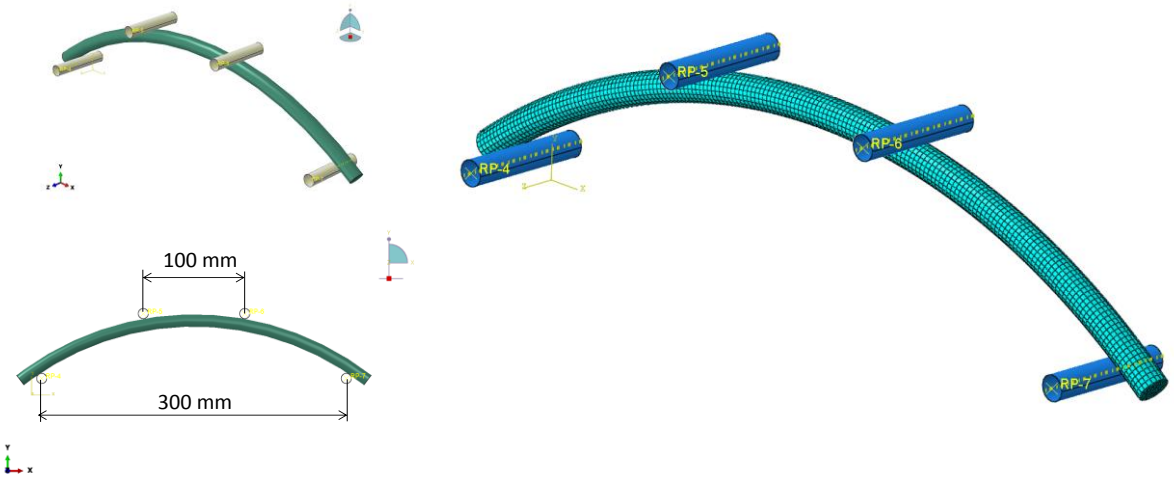

Figure 3: Details of the finite element model used to simulate four-point bending test.

4. RESULTS AND DISCUSSION

Figure 4 presents a plot of the load as a function of the displacement for the spirals. The E/PU/S sample shows higher strength, indicating load at rupture 2940 N. It is observed that the FE model had good correlation to the experimental curves. A non-linear behavior was observed in the numerical analysis. In the experimental curves occurs the same behavior occurred, but with lower magnitude. Both samples (E/PU/S and E/FW/S) show failure at the fiber with subsequent delamination. The difference in the displacement occurs because the measurement is done directly by the machine device and not locally in the sample.

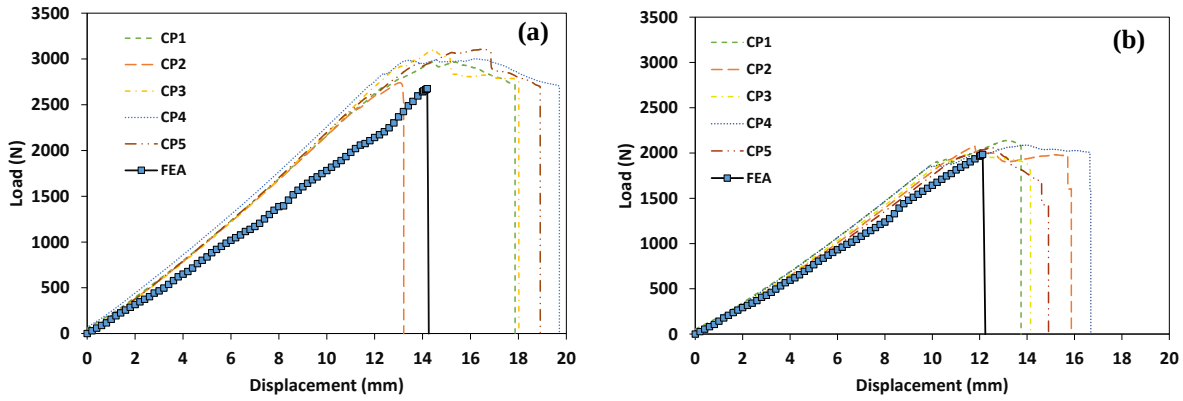

Figure 4: Load *vs.* displacement – numerical and experimental results: (a) E/PU/S and (b) E/FW/S.

In order to validate the values of the parameters of the progressive damage model, a stress vs. strain curve was compared with experimental data. A very good agreement is obtained, as illustrated in Figure 5. The curves represented by points A and B show the strain at the region where the strain gages (SGA and SGB) were bonded. Observe that strains and stresses in point A are positive and in point B are negative, as expected in four point bending. The symmetry between strain in the upper and lower region shows that the sample was subjected to pure bending load. The model was able to predict the behavior of all samples, and the maximum relative difference between numerical and experimental results is 3.5% for stress and 7.9% for strain at rupture. The spirals show fiber failure by compression stress caused by the bending load and locally due the stress concentration caused by the test indenter.

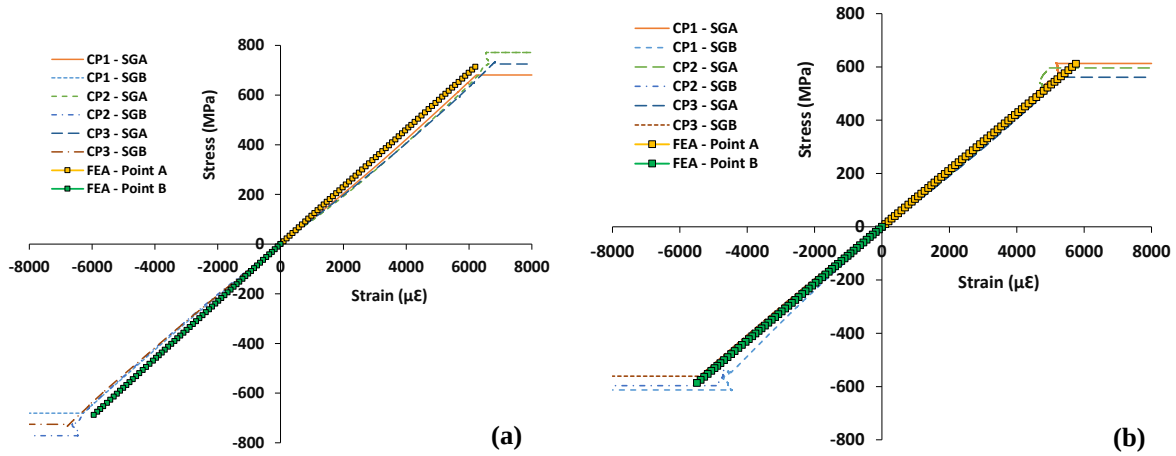

Figure 5: Stress vs. strain – numerical and experimental results: (a) E/PU/S and (b) E/FW/S.

Figure 6(a) presents a plot of the load as a function of the displacement of the samples manufactured with ring section. PPS/FW/R sample shows only delamination and, due to that, the model is less sensitive to identify failure. The E/PU/S shows the highest load at rupture and a more severe damage was found for PPS/FW/R due the delamination. The same behavior is noticed for the stress-strain curve, shown in Figure 6(b).

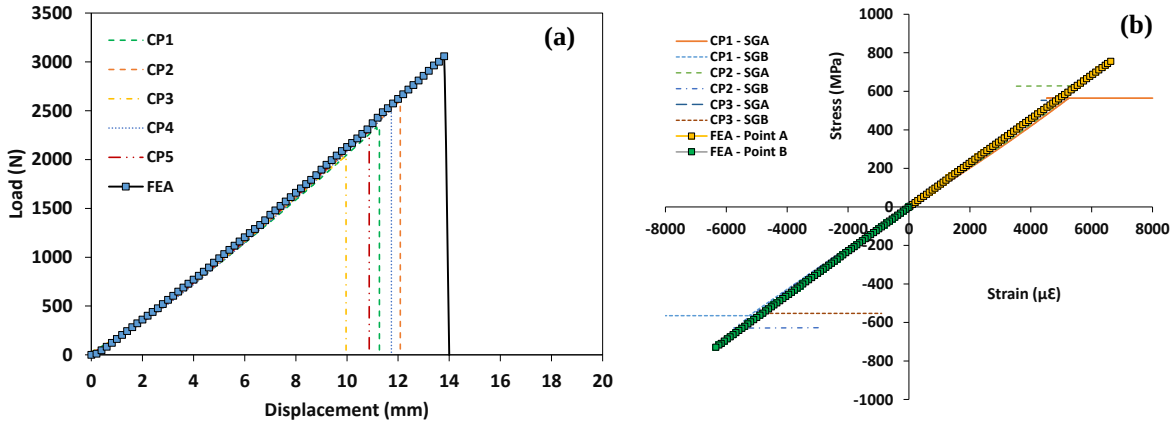

Figure 6: PPS/FW/R: (a) Load *vs.* displacement and (b) Stress *vs.* strain curve.

In accordance to the work published by Ribeiro et al. [4], who evaluated filament wound laminates, for failure under four point bending, it is important to make the model with contact algorithm due to bending-stretching coupling. This phenomenon is even more expressive in these simulations, because the samples are curved. As illustrated in Figure 7, bending-stretching coupling occurs and the model predicts very well this phenomenon. Initial failure is also predicted by the model, and E/PU/S and E/FW/S samples, with high interlaminar strength, show failure closer to the upper device. The PPS/FW/R sample shows damage concentrated in the middle of the beam, justified by sample failure due to delamination caused by transverse shear stresses. Delamination is also reported in the study of Meng et al. [9].

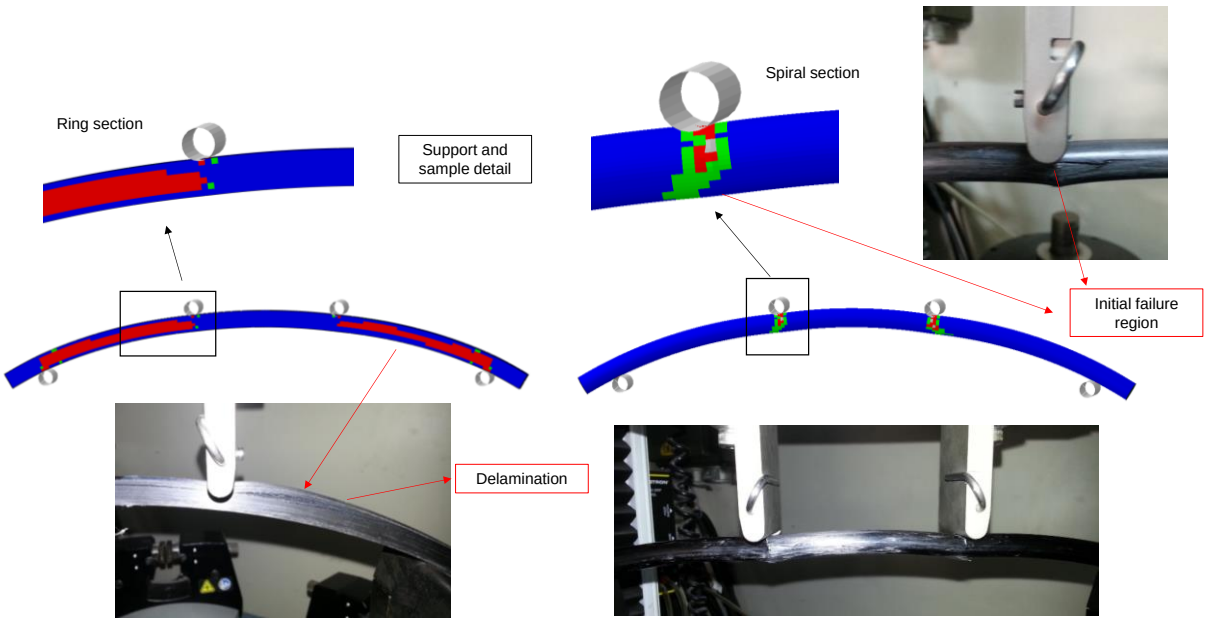

Figure 7: Progressive damage analysis and experimental failure comparison.

As the results shows, the model has excellent accuracy, but it has difficulty in detecting some secondary behavior in the experiments. The load vs displacement curves of the spiral samples do not show a well defined maximum peak, while the numerical results shows an abrupt load drop. This behavior occurs in the experiment due to local failure in the sample. Another restriction of the model is capacity to predict of the delamination in samples manufactured by filament winding as the

PPS/FW/R. This behavior has relation with type of the manufacture process. Previous study has demonstrated the quality and fiber distribution in these composites [10]. The ring manufactured by filament winding presented the areas rich in resin between the layers well organized, while the spiral manufactured by curved pultrusion process presented random areas rich in resin. This characteristic is originated due the ring manufactured by filament winding has layers and the spiral manufactured by pultrusion is make with unique rod. This correlation is expressed in four-point bending test due the areas rich in resin of the ring are in the same direction of the out-plane shear stress or transverse shear stress caused by shear load originated in bending load. The model did not consider these areas rich in resin between layers. Rich areas in resin with randomly distributed improves the strength of the spiral, preventing the failure occurs by delamination at first.

5. CONCLUSIONS

Sections of composite spiral and rings have been analyzed. A composite material model of the curved structures using damage model has been validated comparing simulation and four-point bending results. The difference between numerical and experimental results was 3.5% at maximum stress. Therefore, the finite element model can be applied in other simulations of the curved pultruded and curved filament wound composites with good accuracy. Due to the curved geometry of these structures, the model is sensitive to bending-stretching coupling and this can also delay convergence, and there is a correlation with the stress concentration effects caused by the sample-test device contact. Another important conclusion is that the model identified stress field and failure region for all samples. Experimental results of the spirals manufactured by pultrusion and filament winding failed mainly due to compressive stress and delamination. In addition, the rings manufactured by filament winding showed a higher evidence of delamination, which is linked to their interlaminar strength.

ACKNOWLEDGEMENTS

The authors gratefully acknowledge Petrobras for the development and financial support of this work. Also CNPq and Propesq for research support.

REFERENCES

[1] E.J. Barbero, *Finite Element Analysis of Composite Materials using Abaqus™*, CRC Press, 1st Edition, Boca Raton, 2013.

[2] L. Rampi, P. Lavagna, TRELLINE™ – A Cost-Effective Alternative for Oil Offloading Lines (OOLs), *Proceedings of the Offshore Technology Conference 2006 - OTC*, Houston, pp.1-11, 2006.

[3] T. Lassen, A. I. Lem, G. Imingen, Load response and finite element modelling of bonded offshore loading hoses, *Proceedings of the 33º International conference on ocean offshore and arctic engineering OMAE 2014*, San Francisco, pp. 1-17, 2014.

[4] M.L. Ribeiro, D. Vandepitte, V. Tita, Damage model and progressive failure analyses for filament wound composite laminates, *Applied Composite Materials*, **20**, pp. 975-992, 2013.

[5] M. Bruyneela, J.P. Delsemme, A.C. Goupila, P. Jetteur, C. Lequesne, T. Naito, Y. Urushiyama, Damage modeling of laminated composites: validation of the intra_laminar law of SAMCEF at the coupon level for ud plies, *Proceedings of the 16th European conference on composite materials*, Seville, pp. 22-26, 2014.

[6] J.S. Mayes, A.C. Hansen, Composite laminate failure analysis using multicontinuum theory, *Composites Science and Technology*, **64**, pp. 379–394, 2003.

[7] J.H.S. Almeida Jr., M.L. Ribeiro, V. Tita, S.C. Amico, Damage and failure in carbon/epoxy filament wound composite tubes under external pressure: Experimental and numerical approaches, *Materials and Design*, **96**, pp. 431–438, 2016.

[8] M.L.P Tonatto, R. Teles, M.M.C Forte, V. Tita, S.C Amico, Analysis of carbon fiber composite coil and ring for offloading hoses under crushing load via computational modelling, *Proceedings of the 20th International Conference on Composite Materials*, Copenhagen, pp. 1-10, 2015.

[9] M. Meng, H.R. Le, M.J. Rizvi, S.M. Grove, 3D FEA modelling of laminated composites in bending and their failure Mechanisms, *Composite Structures*, **119**, pp. 693-708, 2015.

[10] M.L.P Tonatto, E. Kerche, M.M.C Forte, S.C Amico, Avaliação da resistência interlaminar em perfis curvos de material compósito com fibra de carbono por ensaio short beam, *Proceedings of the 13th Congresso brasileiro de polímeros*, Natal, pp. 1-4, 2015.